ChemComm

COMMUNICATION

View Article Online
View Journal | View Issue

Cite this: *Chem. Commun.*, 2017, 53, 3890

Received 11th January 2017,
Accepted 14th March 2017

DOI: 10.1039/c7cc00244k

rsc.li/chemcomm

Spontaneous and specific binding of enterohemorrhagic *Escherichia coli* to overoxidized polypyrrole-coated microspheres†

Xueling Shan,[a] Takuya Yamauchi,[a] Yojiro Yamamoto,[ab] Saroh Niyomdecha,[ac] Kengo Ishiki,[a] Dung Q. Le,[a] Hiroshi Shiigi*[a] and Tsutomu Nagaoka[a]

Specific identification of enterohemorrhagic *Escherichia coli* was achieved using microspheres coated with overoxidized polypyrrole. The microspheres are well dispersed in aqueous media, and they specifically, spontaneously, and efficiently bind *E. coli* O157:H7 through surface area effects. In addition, we found that light-scattering by a single microsphere depended linearly on the number of bound cells.

The "lock and key" concept[1] has been exploited to engineer useful molecules such as antibiotics,[2] enzymes,[3] supramolecules,[4] and molecularly imprinted polymers[5] with artificial cavities that complement and thereby recognize small molecules. However, recent studies have highlighted the importance of detecting larger and more complex targets to fuel advances in biology, medical care, drug discovery, and public health.[6] For such applications, cell imprinting on functionalized surfaces enables customization for various target cells.[7] Most cell-imprinted polymers are formed on planar substrates such as electrodes and chips and recognize target cells with good sensitivity and selectivity.[8] However, it is often necessary to couple these devices with dielectrophoresis,[9] microfluidics,[10] and other supplementary technologies to enhance the binding affinity. Some studies on cell imprinting have focused on 3-dimensional (3D) microbeads[11] that can recognize target cells spontaneously by size and shape effects. These studies present an imaginative method using Pickering emulsion for preparing cell-imprinted microbeads. However, these also cause environmental problems because they require the use of organic solvents and the size of the microbead is >100 μm.

To overcome these problems, here we fabricated a cell-imprinted microsphere in an aqueous medium and found that high binding affinity can be achieved without additional technologies by increasing the surface area of the substrate and thereby enhancing the flow.

We fabricated cell-imprinted microspheres complementary to *Escherichia coli* O157:H7 in an aqueous medium. The microspheres comprised a micrometer-scale core and a polymer complex shell; the core was a gold-coated plastic microbead (mean diameter: 5.0 μm, see Fig. S1, ESI†), as shown in Fig. 1A.[12] A self-assembled aminothiophenol monolayer (SAM) was first deposited on the core surface and coated with Nafion through electrostatic interactions.[13] Polypyrrole (PPy) was then

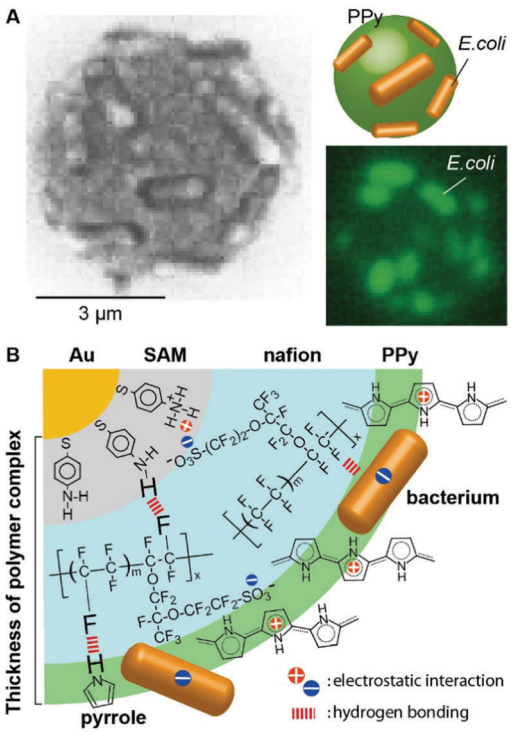

Fig. 1 (A) SEM and fluorescence images of the microsphere coated with the *E. coli*-doped polymer complex and (B) schematic illustration of the structure of the polymer complex.

[a] *Department of Applied Chemistry, Osaka Prefecture University, 1-2 Gakuen, Naka, Sakai, Osaka 599-8570, Japan. E-mail: shii@chem.osakafu-u.ac.jp*
[b] *GreenChem. Inc., 19-19 Tsuruta, Nishi, Sakai, Osaka 593-8323, Japan*
[c] *Department of Chemistry, Prince of Songkla University, Hat Yai, Songkla 90112, Thailand*

† Electronic supplementary information (ESI) available: Experimental procedures and supporting figures. See DOI: 10.1039/c7cc00244k

generated on the Nafion-modified surface by chemical oxidation in an aqueous medium containing *E. coli* O157:H7. The SEM image showed that the polymerization occurred preferentially on the surface of the Nafion-coated microbead, since no PPy structure was observed on the substrate. Moreover, we could not observe the formation of PPy on the gold-coated microbead prepared without Nafion (see Fig. S2, ESI†). This suggested that the pyrrole monomer interacted through hydrogen bonds with the fluorine atom of Nafion and the polymerization proceeded only at the surface of the microsphere as a reaction field. We believe that the Nafion-modified core acted as the initial dopant anion, although cells that adhered to the microsphere as polymerization progressed eventually acted as dopant anions with a negative zeta potential of −11 mV (Fig. 1B). Finally, this process generated microspheres decorated with cells (mean diameter: 6.5 μm).

Scanning electron microscopy (SEM) and fluorescence microscopy confirmed that the cells were entrapped in the polymer film. PPy is believed to have been formed on the doped cells as well, since there was no significant difference in the contrast between cells, which are insulators, and the polymer film, which is a conductor. The thickness of the PPy film on a cell was estimated to be about ∼50 nm from SEM observation of original cells (length: 1.99 ± 0.16 μm, width: 0.65 ± 0.15 μm) and doped cells on the microsphere (length: 1.99 ± 0.21 μm, width: 0.66 ± 0.04 μm); it seems that the polymerization of PPy on the cell did not fully progress. To prepare cell-imprinted cavities on the microspheres, it was necessary to optimize the thickness of the polymer complex, which can be controlled by adjusting the amount of Nafion (see Fig. S3, ESI†) and was estimated to be 0.75 μm in the fabricated microspheres.

The microspheres were then incubated for 3 h in aqueous 0.10 M NaOH to overoxidize PPy through curing and dedoping.[14] This reaction efficiently removed the imprinted cells from the shell and thereby exposed bacilli-like surfaces complementary to *E. coli* (Fig. 2A). As a matter of course, the bacteria died in a strong alkali medium (pH 13). It was confirmed that the OD600 value of the *E. coli* O157:H7 suspension decreased from 0.24 to 0.040 after 3 hours of incubation. Since lipopolysaccharides, hydrophobic lipid moieties and membrane proteins in the outer membrane were damaged and denatured, the outer membranes of cells were broken and disassembled (see Fig. S4, ESI†). At that time, the thinner PPy film on the cells might also be decomposed. Therefore, it is expected that the removal of cells from the PPy microsphere proceeded by the overoxidation process. On average, 10 such cavities were observed by SEM on the top hemisphere of a single microsphere ($n > 100$), and no bacteria remained. Notably, cracking and peeling of the polymer film were not observed after overoxidation, suggesting that Nafion is sufficiently adhesive and forms a structurally robust intertwined network with PPy.

Two milligrams (1.6×10^7 microspheres) of the imprinted microspheres were then incubated for 3 h in a suspension of *E. coli* O157:H7 (6.0×10^7 cells) in 3.0 mL phosphate buffer. Subsequently, the microspheres were precipitated by gravity and were found to have captured *E. coli* cells in complementary cavities without adsorption to smooth surfaces (Fig. 2B).

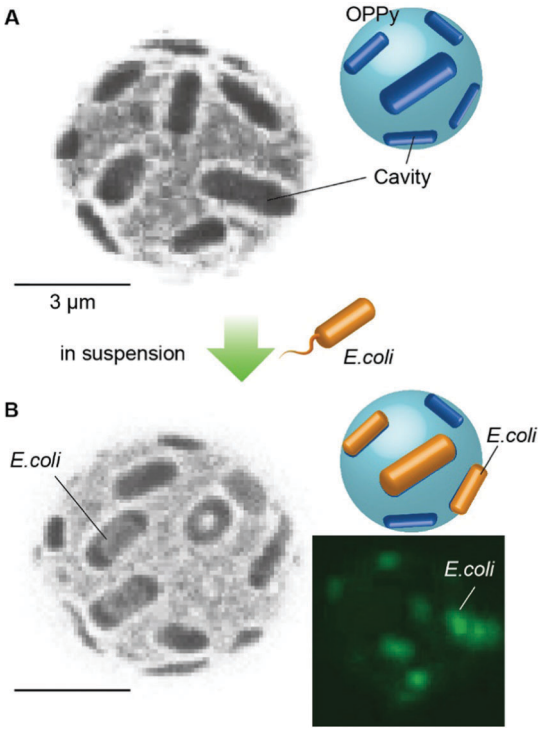

Fig. 2 SEM and fluorescence images of an *E. coli* cell-imprinted microsphere (A) before and (B) after testing against SYTO9-stained *E. coli*. Bars in the SEM images are 3 μm.

Thus, the microspheres captured cells spontaneously without the need for additional technologies.

Binding of *E. coli* O157:H7 was confirmed using 5′-bi-1*H*-benzimidazole (BI: Hoechst 33258), a fluorescent label that intercalates into the minor groove of double-stranded bacterial DNA.[15] A mixture of fluorescent-labeled *E. coli* O157:H7 (3.6×10^8 cells) and the imprinted microspheres (2.0 mg) was then incubated at 298 K for 30 min, after which the microspheres were precipitated by gravity. The fluorescence intensity of the supernatant (I) at 497 nm was drastically lower than that of an *E. coli* O157:H7 suspension without microspheres (I_0) (inset in Fig. 3A). The normalized intensity $(I_0 - I)/I_0$, a measure of the fraction of *E. coli* O157:H7 cells captured by the microspheres, was constant at around 0.8 against 10^6–10^8 cells (Fig. 3B), suggesting that the microspheres bound about 80% of the cells.

Spontaneous and selective binding of target cells is critical for real-world applications. Hence, we tested the microspheres against suspensions containing 6.0×10^7 *E. coli* O157:H7, *E. coli* O157:HNM, *E. coli* O26:H11, *E. coli* O26:HNM, *E. coli* O rough, *Pseudomonas aeruginosa*, *Serratia marcescens*, and *Acinetobacter calcoaceticus* cells. After incubation for 3 h, the number of cells remaining in the supernatant (n) was quantified using the cell counting methods described in the Experimental section (Fig. 3C). Uptake (s) was calculated as $(n_0 - n)/n_0$, where n_0 is the initial number of cells. The uptake for *E. coli* O157:H7 (s_0) was the highest among all the strains, thus highlighting the specificity of the microspheres, with $s/s_0 < 0.1$. The specificity of the imprinted microspheres arises from the shape and size complementarity to

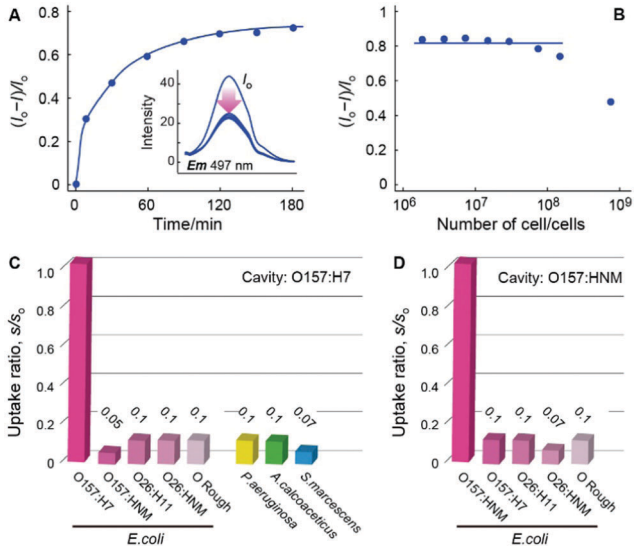

Fig. 3 (A) Time course of the binding of bacterial cells (3.6×10^8 cells) to 2.0 mg of cell-imprinted microspheres. The normalized intensity $(I_0 - I)/I_0$ was calculated from the supernatant intensity (I) and the intensity of the initial suspension (I_0). Inset, time dependence of the fluorescence spectra at an excitation wavelength of 352 nm. (B) Plot of $(I_0 - I)/I_0$ *vs.* number of cells in the suspension (3.0 mL). (C) Uptake ratio (s/s_0) of the microspheres imprinted with *E. coli* O157:H7, where s is the uptake for a test strain, and s_0 is the uptake for *E. coli* O157:H7. Uptake (s) was calculated as $(n_0 - n)/n_0$ from the number of cells in the initial suspension (n_0) and in the supernatant after incubation with the microspheres (n). (D) Uptake ratio (s/s_0) of the microspheres imprinted with *E. coli* O157:HNM.

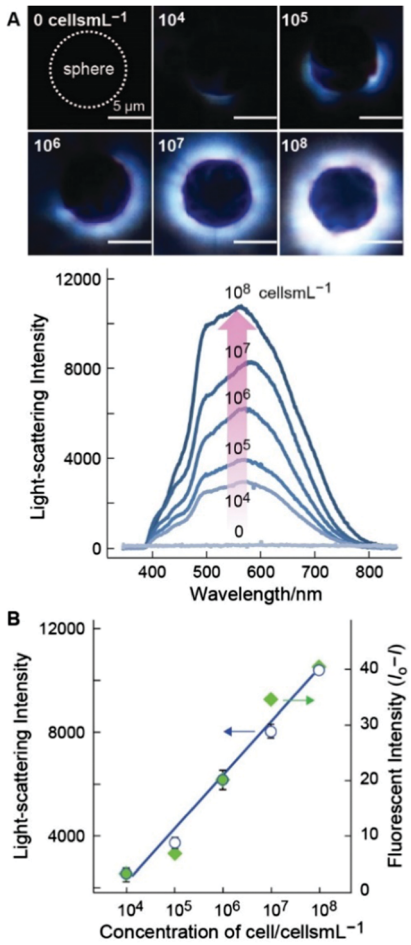

Fig. 4 (A) Dark-field microscopic images and light-scattering spectra of a cell-imprinted microsphere after incubation with the indicated concentration of *E. coli* O157:H7. Scale bars in the dark-field images are 5 μm. (B) Relationship between light-scattering intensity of a single microsphere and fluorescence intensity ($I_0 - I$) of captured cells.

E. coli O157:H7 as well as from the chemical structure of the cavity surface. The polymer complex coat was likely provided with an array of functional groups including sulfo, fluoro, hydroxyl, carbonyl, carboxyl, amino, and imino groups corresponding to the surface chemical structure of target cells on the inner surface of the shape-complementary cavity. Therefore, we hypothesized that the microspheres interact with the target cells at multiple points. Notably, the microspheres distinguished strongly between motile *E. coli* O157:H7 and non-motile *E. coli* O157:HNM, which have the same O antigen but different H antigens. In an effort to explain the selectivity between these two strains we also prepared *E.coli* O157:HNM cell-imprinted microspheres. The microspheres indicated a high selective characteristic to *E.coli* O157:HNM as well (Fig. 3D). There was no significant difference in the selectivity between microspheres imprinted with *E.coli* O157:H7 and those imprinted with *E.coli* O157:HNM. This result suggested that the distribution of functional groups on their surface differ among different *E.coli* strains, which makes them particular in the surface chemical structure while they have the same O antigen. We also found the difference in the size of cells between *E. coli* O157:H7 (length: 1.99 ± 0.16 μm, width: 0.65 ± 0.15 μm) and *E. coli* O157:HNM (length: 2.06 ± 0.36 μm, width: 0.71 ± 0.11 μm). Therefore, the cavities of *E.coli* O157:H7 and *E.coli* O157:HNM have different shapes and binding sites corresponding to the surface chemical structure of target cells on their inner surfaces; consequently, the cell-imprinted microspheres can specifically identify target cells.

Previously, we reported that a plastic microbead fully coated with metal does not scatter light under a dark-field microscope.[16] Consistent with this, in this study, we found that the cell-imprinted microspheres did not scatter light, with intensity ≅0 under the same experimental conditions (Fig. 4A). After incubation with a suspension of 3.0×10^4 bacterial cells, some light scattering was observed with an intensity of 2950 at 560 nm. The light-scattering intensity increased drastically with cell density and reached 11 000 at 3.0×10^8 cells. Light is weakly scattered due to a small difference in the refractive index between the surrounding air (1.0) and water (1.3) inside a cell,[17] and we found this scattering to be 1550 (n = 10) for a single cell (see Fig. S5A, ESI†). Accordingly, we estimated that 4–15 cells were captured per microsphere after incubation with 3.0×10^4–3.0×10^8 cells, while noting that the light-scattering intensity was dependent on the number of cells bound to the bottom hemisphere. Since we approximated from SEM images that an imprinted microsphere contains 20 cavities, this result suggested that at least 70% of the cavities were occupied in a suspension of 3.0×10^8 cells. Fig. 4B showing light scattering by a cell-imprinted microsphere after

incubation in various concentrations of *E. coli* O157:H7 highlights the apparent equilibrium between cavities and cells as well as the strong correlation between light scattering and the fluorescence intensity of captured cells.

In summary, we engineered a water-dispersible microsphere with shape complementarity to *E. coli* O157:H7. The microsphere was coated with Nafion to generate a layer of PPy in the presence of *E. coli*. The polymer was then overoxidized by curing and dedoping to expose surfaces that specifically and spontaneously bind *E. coli* O157:H7 through surface area effects. The microsphere scattered light is in linear proportion to the number of captured cells. We believe that the microsphere can be useful not only to concentrate target cells efficiently but also to specifically detect targets such as food-poisoning bacteria, pathogens, and hygiene indicators. Our approach may also enable rapid development (within a few days) of devices for specifically detecting new and unforeseen bacterial threats, since the cavities can be tailor-made on the microspheres. The simplicity of fabrication allows the integration of this system into various devices that could then be produced at an industrial scale without pre-concentration, purification, and laborious synthesis, unlike immunological methods that require over a month to develop. Finally, the imprinted ultrastructure is also a micrometer-scale environment that sustains cell viability, and thus may provide many new possibilities in basic and applied life science research.

We thank Professor M. Miyake of Osaka Prefecture University and Dr K. Seto of Osaka Prefectural Institute of Public Health for providing verotoxin-nonproducing *E. coli*. This work was supported by the Ministry of Agriculture, Forestry, and Fisheries through a science and technology research promotion program for the agriculture, forestry, fisheries, and food industries. We also acknowledge financial support from the Japan Society for the Promotion of Science through Grants-in-Aid for Scientific Research (B) (KAKENHI 25288039, 16H04137) and Grant-in-Aid for Challenging Exploratory Research (KAKENHI 26620072). X. S. acknowledges the financial support received from the Otsuka Toshimi Scholarship Foundation through a Grant-in-Aid for the scholarship recipient.

Notes and references

1 (*a*) E. Fischer, *Ber. Dtsch. Chem. Ges.*, 1894, **27**, 2985; (*b*) I. Gill and A. Ballesteros, *J. Am. Chem. Soc.*, 1998, **120**, 8587.
2 (*a*) J. L. Urraca, A. J. Hall, M. C. Moreno-Bondi and B. Sellergren, *Angew. Chem.*, 2006, **118**, 5282; (*b*) R. Bouley, M. Kumarasiri, Z. Peng, L. H. Otero, W. Song, M. A. Suckow, V. A. Schroeder, W. R. Wolter, E. Lastochkin, N. T. Antunes, H. Pi, S. Vakulenko, J. A. Hermoso, M. Chang and S. Mobashery, *J. Am. Chem. Soc.*, 2015, **137**, 1738.
3 (*a*) D. J. Caruana and A. Heller, *J. Am. Chem. Soc.*, 1999, **121**, 769; (*b*) E. A. Schilling, A. E. Kamholz and P. Yager, *Anal. Chem.*, 2002, **74**, 1798; (*c*) G. Liu, Y. Wan, V. Gau, J. Zhang, L. Wang, S. Song and C. Fan, *J. Am. Chem. Soc.*, 2008, **130**, 6820.
4 (*a*) E. Golub, G. Pelossof, R. Freeman, H. Zhang and I. Willner, *Anal. Chem.*, 2009, **81**, 9291; (*b*) R. Freeman, E. Sharon, R. Tel-Vered and I. Willner, *J. Am. Chem. Soc.*, 2009, **131**, 5028; (*c*) B. Sellergren, *Nat. Chem.*, 2010, **2**, 7.
5 (*a*) M. J. Whitecombe and E. N. Vulfson, *Adv. Mater.*, 2001, **13**, 467; (*b*) J. L. Urraca, C. S. A. Aureliano, H. Schillinger, H. Esselmann, J. Wiltfang and B. Sellergren, *J. Am. Chem. Soc.*, 2011, **133**, 9220; (*c*) A. Poma, A. Guerreiro, M. J. Whitcombe, E. V. Piletska, A. P. F. Turner and S. A. Piletsky, *Adv. Funct. Mater.*, 2013, **23**, 2821; (*d*) A. G. Ayankojo, A. Tretjakov, J. Reut, R. Boroznjak, A. Öpik, J. Rappich, A. Furchner, K. Hinrichs and V. Syritski, *Anal. Chem.*, 2016, **88**, 1476.
6 (*a*) W. Cheng, L. Ding, S. Ding, Y. Yin and H. Ju, *Angew. Chem., Int. Ed.*, 2009, **48**, 6465; (*b*) A. Aherne, C. Alexander, M. J. Payne, N. Perez and E. N. Vulfson, *J. Am. Chem. Soc.*, 1996, **118**, 8771; (*c*) H. Shiigi, S. Tokonami, H. Yakabe and T. Nagaoka, *J. Am. Chem. Soc.*, 2005, **127**, 3280.
7 (*a*) S. Sykora, A. Cumbo, G. Belliot, P. Pothier, C. Arnal, Y. Dudal, P. F.-X. Corvini and P. Shahgaldian, *Chem. Commun.*, 2015, **51**, 2256; (*b*) K. Ren and R. N. Zare, *ACS Nano*, 2012, **6**, 4314.
8 (*a*) M. Mahmoudi, S. Bonakdar, M. A. Shokrgozar, H. Aghaverdi, R. Hartmann, A. Pick, G. Witte and W. J. Parak, *ACS Nano*, 2013, **7**, 8379; (*b*) T. Wangchareansak, A. Thitithanyanont, D. Chuakheaw, M. P. Gleeson, P. A. Lieberzeit and C. Sangma, *J. Mater. Chem. B*, 2013, **1**, 2190.
9 S. Tokonami, Y. Nakadoi, M. Takahashi, M. Ikemizu, T. Kadoma, K. Saimatsu, L. Q. Dung, H. Shiigi and T. Nagaoka, *Anal. Chem.*, 2013, **85**, 4925.
10 (*a*) K. Ren, N. Banaei and R. N. Zare, *ACS Nano*, 2013, **7**, 6031; (*b*) M. Darder, P. Aranda, L. Burgos-Asperilla, A. Llobera, V. J. Cadarso, C. Fernández-Sánchez and E. Ruiz-Hitzky, *J. Mater. Chem.*, 2010, **20**, 9362.
11 (*a*) X. Shen, J. S. Bonde, T. Kamra, L. Bülow, J. C. Leo, D. Linke and L. Ye, *Angew. Chem.*, 2014, **126**, 10863; (*b*) P. Wongkongkatep, K. Manopwisedjaroen, P. Tiposoth, S. Archakunakorn, T. Pongtharangkul, M. Suphantharika, K. Honda, I. Hamachi and J. Wongkongkatep, *Langmuir*, 2012, **28**, 5729.
12 (*a*) H. Shiigi, S. Shirai, T. Fujita, H. Morishita, Y. Yamamoto, T. Nishino, S. Tokonami, H. Nakao and T. Nagaoka, *J. Electrochem. Soc.*, 2013, **160**, H630; (*b*) S. Tokonami, Y. Yamamoto, Y. Mizutani, I. Ota, H. Shiigi and T. Nagaoka, *J. Electrochem. Soc.*, 2009, **156**, D558; (*c*) Y. Yamamoto, S. Takeda, H. Shiigi and T. Nagaoka, *J. Electrochem. Soc.*, 2007, **154**, D462.
13 (*a*) G. He, Z. Li, Y. Li, Z. Li, H. Wu, X. Yang and Z. Jiang, *ACS Appl. Mater. Interfaces*, 2014, **6**, 5362; (*b*) K. A. Mauritz and R. B. Moore, *Chem. Rev.*, 2004, **104**, 4535.
14 (*a*) S. Tokonami, H. Shiigi and T. Nagaoka, in *Molecularly Imprinted Sensors: Overview and Applications*, ed. S. Li, Y. Ge, S. A. Piletsky and J. Lunec, Elsevier B. V., Amsterdam, 2012, pp. 73–89; (*b*) H. Shiigi, D. Kijima, Y. Ikenaga, K. Hori, S. Fukazawa and T. Nagaoka, *J. Electrochem. Soc.*, 2005, **152**, H129.
15 (*a*) N. Busto, B. Cano, R. Tejido, T. Biver, J. M. Leal, M. Venturini, F. Secco and B. García, *J. Phys. Chem. B*, 2015, **119**, 4575; (*b*) A. Burmistrova, B. Fresch, D. Sluysmans, E. De Pauw, F. Remacle and A.-S. Duwez, *Nanoscale*, 2016, **8**, 11718.
16 (*a*) H. Shiigi, S. Kimura, T. Fujita and T. Nagaoka, *Anal. Sci.*, 2015, **31**, 577; (*b*) H. Shiigi, T. Fujita, X. Shan, M. Terabe, A. Mihashi, Y. Yamamoto and T. Nagaoka, *Anal. Sci.*, 2016, **32**, 281.
17 (*a*) H. Shiigi, M. Fukuda, T. Tono, K. Takada, T. Okada, L. Q. Dung, Y. Hatsuoka, T. Kinoshita, M. Takai, S. Tokonami, H. Nakao, T. Nishino, Y. Yamamoto and T. Nagaoka, *Chem. Commun.*, 2014, **50**, 6252; (*b*) H. Shiigi, T. Kinoshita, M. Fukuda, L. Q. Dung, T. Nishino and T. Nagaoka, *Anal. Chem.*, 2015, **87**, 4042; (*c*) Z. Fang, Y. Zhen, O. Neumann, A. Polman, F. J. G. Abajo, P. Nordlander and N. J. Halas, *Nano Lett.*, 2013, **13**, 1736.

Electronic Supplementary Information

Spontaneous and specific binding of enterohemorrhagic *Escherichia coli* to overoxidized polypyrrole-coated microspheres

Xueling Shan,[a] Takuya Yamauchi,[a] Yojiro Yamamoto,[a,b] Saroh Niyomdecha,[a,c] Kengo Ishiki,[a] Dung Q. Le,[a] Hiroshi Shiigi,*[a] and Tsutomu Nagaoka[a]

[a]Department of Applied Chemistry, Osaka Prefecture University, 1-2 Gakuen, Naka, Sakai, Osaka 599-8570, Japan. E-mail: shii@chem.osakafu-u.ac.jp

[b]GreenChem. Inc., 19-19 Tsuruta, Nishi, Sakai, Osaka 593-8323, Japan.

[c]Department of Chemistry, Prince of Songkla University, Hat Yai, Songkla 90112, Thailand.

*To whom correspondence should be addressed. E-mail: shii@chem.osakafu-u.ac.jp

Table of Contents

Experimental

Chemicals. All chemicals were reagent grade. Ultrapure water (> 18 MΩ cm) sterilized with UV light was used in all experiments. For safety reasons, experiments were conducted with genetically modified verotoxin-nonproducing *Escherichia coli* PV856 (O157:H7), *E. coli* PV276 (O157:HNM), *E. coli* PV01-198 (O26:H11), and *E. coli* PV03-017 (O26:HNM). These strains were provided by Prof. M. Miyake, Department of Veterinary Science, Graduate School of Life and Environmental Sciences, Osaka Prefecture University, and by Dr. K. Seto, Osaka Prefectural Institute of Public Health. *E. coli* K-12 (O Rough:H48, NBRC3301), *P. aeruginosa*, *S. marcescens*, and *A. calcoaceticus* were purchased from National Institute of Technology and Evaluation Biological Resource Center (NBRC).

SYTO9® and Hoechst 33258 (5'-bi-1H-benzimidazole trihydrochloride) were used as fluorescent dyes. Nafion®117 was purchased from Sigma-Aldrich, while gold-coated microbeads were purchased from GreenChem. Inc.[1]

Bacterial culture. Bacterial cultures and experiments were executed in a biosafety level 2 laboratory designed and managed in accordance with safety regulations. Liquid cultures were grown at 303 K for 18 h in E-MC35 agar broth (Eiken Chemical Co. Japan). Similarly, colonies were suspended in 30 mL E-MC35, and cultured at 303 K for 18 h. Cells were then harvested by centrifugation at 7,000 *g* for 15 min and washed four times for 1 min each in fresh phosphate buffer.

Apparatus. Samples were imaged on a TM3030 (Hitachi, Japan) scanning electron microscope operating at accelerating voltage 5 kV, and on a BX51 fluorescent microscope (Olympus, Japan). Fluorescent spectra were collected on FP-6300 (Jasco, Japan).

Fabrication of microspheres imprinted with bacterial cells. Gold-coated microbeads (5 mg), the surface of which was modified with a self-assembled aminothiophenol monolayer, were dispersed in 20 mL 25 vol% aqueous ethanol containing 1-50 µL 20 % nafion. After ultrasonication for 20 min, the dispersion was immediately mixed with 30 µL pyrrole and 5 mL *E. coli* O157:H7 (3.8×10^9 cells mL^{-1}), and stirred for 40 min. Subsequently, polymerization was induced by oxidation with $(NH_4)_2S_2O_8$ for 12 hours at room temperature. Polymer-coated microspheres were then collected by centrifugation at 1,500 *g*, and washed with ultrapure water. To remove bacterial cells, microspheres were redispersed in aqueous 0.1 M NaOH, stirred for 3 hours, washed with ultrapure water, and dried in a vacuum chamber.

Dark-field microscopy. In dark-field microscopy, scattered light is detected, while directly transmitted light is blocked with a dark-field condenser. Samples were thus imaged using an Eclipse 8oi optical microscope (Nikon, Japan) equipped with a dark-field condenser, a 100 W halogen lamp, and a charge-coupled device camera. Light-scattering spectra were obtained using a USB4000 miniature grating spectrometer (Ocean Optics) coupled to the microscope via an optical fiber with core diameter 400 μm.[2] Typical acquisition times were 400 ms. Spectra were corrected for spectral variations in system response, and white-light intensity distribution (main intensity 600 nm) through division by bright-field spectra was recorded through the sample. The collection volume was nearly diffraction-limited for the 100× objective (NA 0.9)/fiber combination used, with cross-sectional area approximately ~10 μm^2. Samples were prepared by mounting on a glass slide 5 μL microspheres, bacterial suspensions, and mixtures thereof, and air drying for 1 hour.

Cell counting. Microspheres imprinted with *E. coli* O157:H7 (2.0 mg) were incubated with 2.0×10^7 cells mL^{-1} of SYTO9-stained *E. coli* O157:H7, O157:HNM, O26:H11, O26:HNM, O rough, *P. aeruginosa*, *S. marcescens*, and *A. calcoaceticus*. After incubation for 3 hours, 5 μL of the supernatant cleared by gravity was mounted on a glass slide, and imaged on a fluorescent microscope to count the number of cells remaining in the presence (n) or absence of microspheres (n_0).

Results

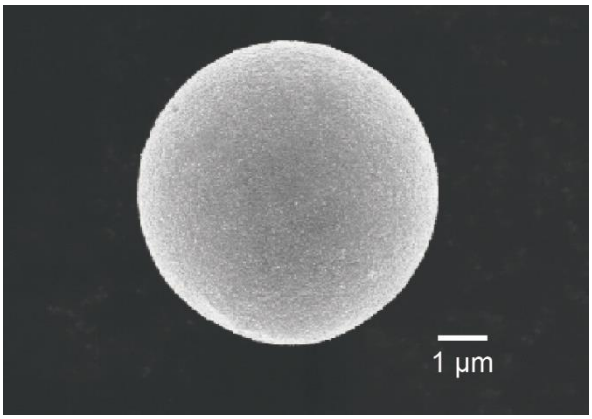

Fig. S1 SEM image of gold-coated acrylic resin microsphere.

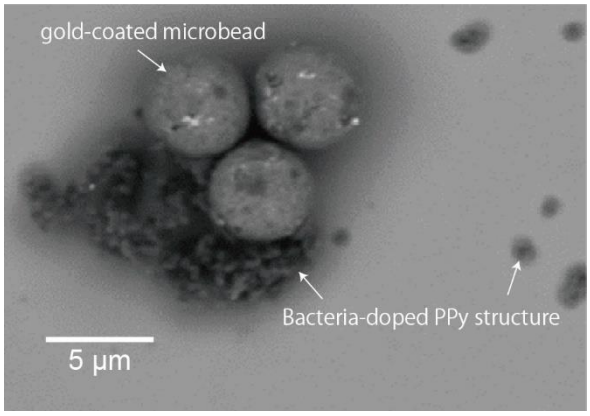

Fig. S2 SEM image of microspheres prepared without nafion.

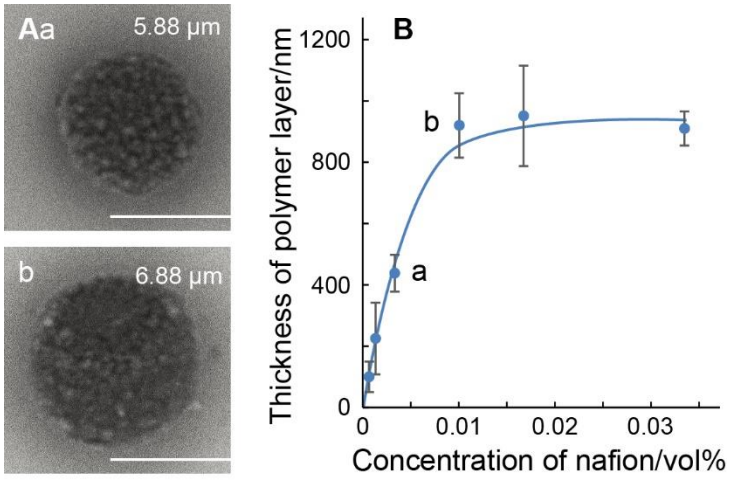

Fig. S3 (A) SEM images of microspheres prepared with (a) 0.0030 and (b) 0.010 vol% nafion. Average diameters are indicated (n = 10). The scale bars in SEM images are 5 μm. (B) Thickness of the polymer complex without cells as a function of nafion concentration.

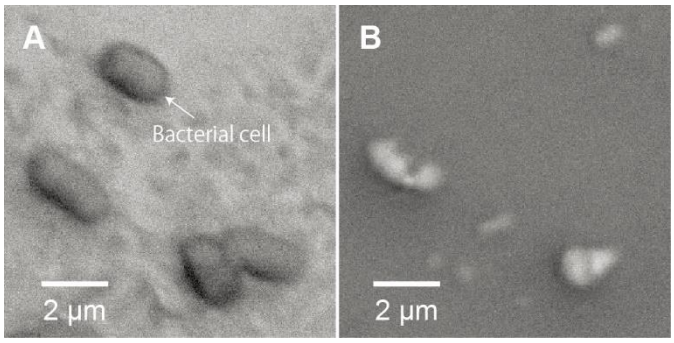

Fig. S4 SEM images of *E. coli* O157:H7 (A) before and (B) after incubation for 3 h in an aqueous 0.10 M NaOH.

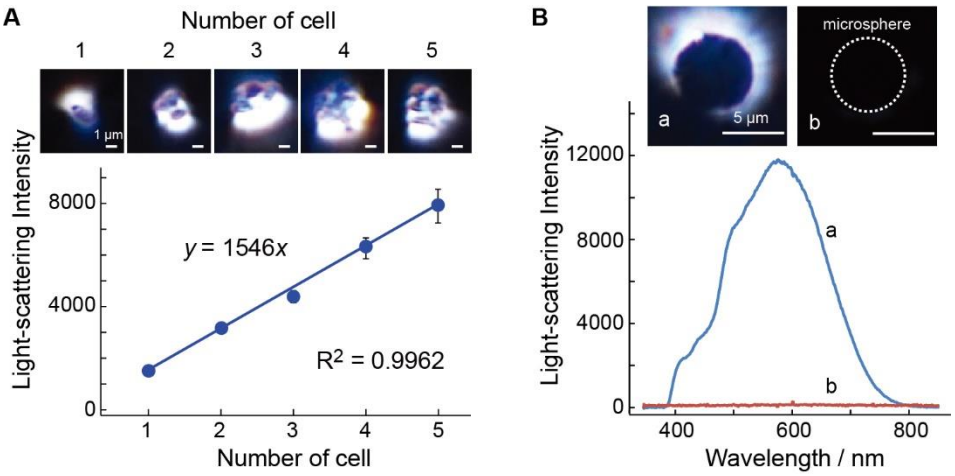

Fig. S5 (A) Dark-field images and light-scattering intensity of *E.coli* O157:H7 cells at different aggregation numbers. The scale bars in dark-field images are 1 μm (n = 10). (B) Dark-field images and light-scattering spectra of a single microsphere (a) before and (b) after doped bacteria are removed. The scale bars in dark-field images are 5 μm (n = 10).

References

1. (a) H. Shiigi, S. Shirai, T. Fujita, H. Morishita, Y. Yamamoto, T. Nishino, S. Tokonami, H. Nakao and T. Nagaoka, *J. Electrochem. Soc.*, 2013, **160**, H630; (b) S. Tokonami, Y. Yamamoto, Y. Mizutani, I. Ota, H. Shiigi, T. Nagaoka, *J. Electrochem. Soc.*, 2009, **156**, D558; (c) Y. Yamamoto, S. Takeda, H. Shiigi, T. Nagaoka, *J. Electrochem. Soc.*, 2007, **154**, D462.
2. (a) H. Shiigi, T. Fujita, X. Shan, M. Terabe, A. Mihashi, Y. Yamamoto, T. Nagaoka, *Anal. Sci.*, 2016, **32**, 281; (b) H. Shiigi, S. Kimura, T. Fujita and T. Nagaoka, *Anal. Sci.*, 2015, **31**, 577.